Proceedings of the
Annual Stability Conference
Structural Stability Research Council
Louisville, Kentucky, April 1-4, 2025

Feasibility study of composite floor system with cold – formed z - sections

Israel Barreto[1], Michael W. Seek[2]

Abstract
Z-sections are used successfully in the metal building industry for purlin and girt systems. They can be nested for efficient lapping and transportation. With automated machines, they can be quickly fabricated from coil stock. Recent research has improved understanding of their flexural behavior. Combining paired Z-sections with bracing creates efficient systems. Heavier Z-sections can be an alternative to W-shapes in composite floor systems. The proposed system can be erected with paired members, metal deck, shear studs, and concrete composite slab. It has the potential to be an efficient solution for composite systems with spans from 30 to 40 feet and can simplify the fabrication process.

1. Introduction

Z-sections have been used very successfully by the metal building industry for purlin and girt systems. One of the main advantages of the Z-section for such systems is that the Z-sections can be nested, which allows for the purlins to be efficiently lapped to provide continuity across the supports and also allows them to be very compactly transported. With automated rolling and punching machines, these members can be quickly and automatically fabricated, starting with coil stock at one end and a finished purlin at the other end, with very little manpower required in between. Z-sections provide a very efficient structural member; however, due to the member's rotated principal axes, they are subject to somewhat complex flexural behavior. Recent research on these systems has dramatically improved understanding of the behavior.

Because Z-sections have rotated principal axes, they will undergo lateral deflection due to a vertically applied (gravity) load. This may be one of the reasons why they have not seen much use in structural systems outside of metal buildings. However, the recent research by Seek and Avci (2024) has shown that by combining purlins in pairs and bracing between them, very efficient systems can be developed. The system proposed herein adopts this philosophy and combines paired Z-sections oriented back-to-back with an x-brace diaphragm applied near the third points of the members as shown in Fig. 1.

[1] Student , Old Dominion University, <ibarr002@odu.edu>
[2] Associate Professor, Old Dominion University, <mseek@odu.edu>

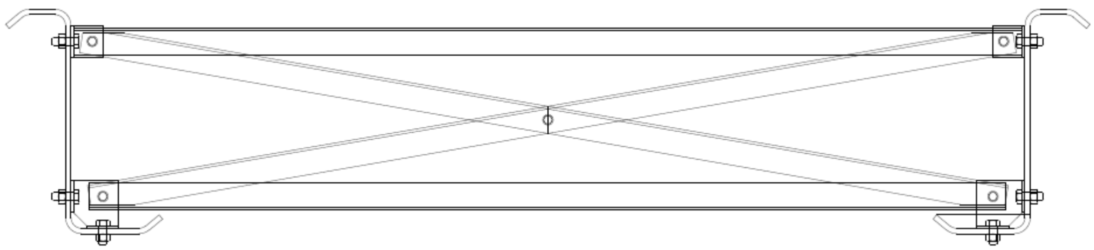

Figure 1: Z-sections oriented back-to-back with an x-brace diaphragm

With the heavier gauge coil stock and forming techniques currently used to make HSS sections, heavier Z- sections (with depths 18” to 24” and thicknesses from 0.1875” to 0.75”) can be developed as an alternative to W-shapes in composite floor systems. Further studies on Z sections may allow for the development of thinner configurations. This proposed system would be erected as follows: (1) Assemble a pair of members on the ground with bracing installed near the third points. (2) Lift the paired members as an assembly using the bracing locations as pick points (3) Drop the members into place (Since the flange of the Z-shape is only on one side of the web they can easily be dropped into position.). (4) Metal deck and shear studs are applied, and concrete composite slab is created by current installation methodologies. A threaded rod could be used to stabilize the ends and provide some alignment adjustment to facilitate connection fit up. There are several end connection configurations that can utilized - a simple shear tab or a partial seat at the top flange for example. The system is inherently stable with two members so with a quick positive connection, the crane can be released for the next pick while the remaining requisite bolts are installed.

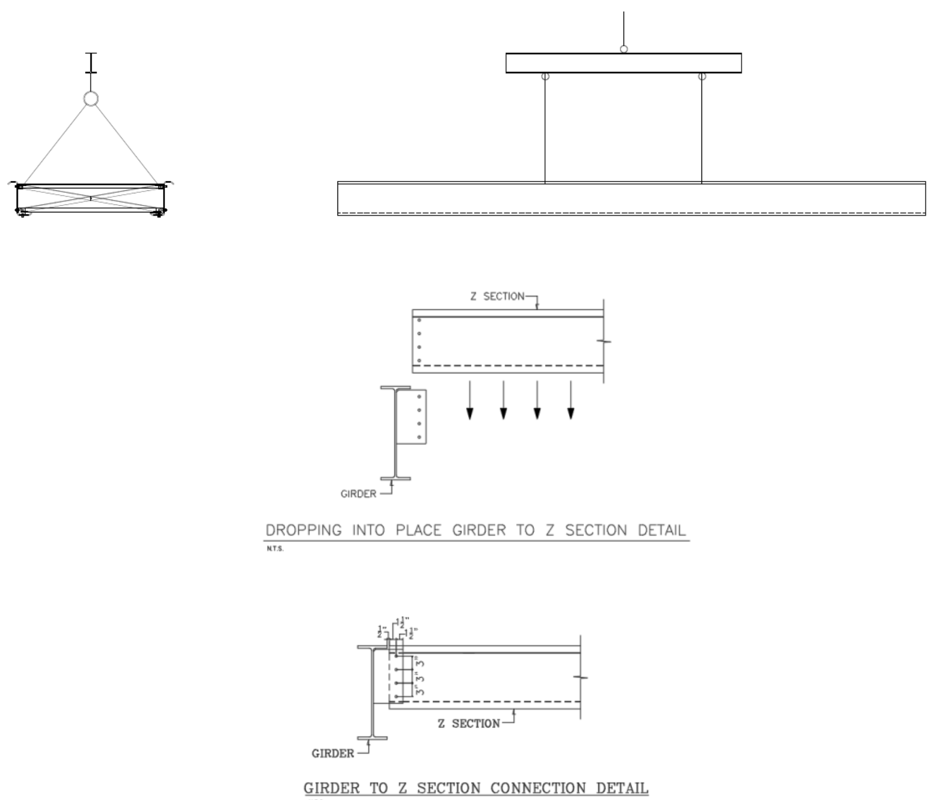

Figure 2: Erection of paired Z-sections

The proposed solution has the potential to be an efficient solution for composite systems with spans from 30 to 40 feet. The systems would allow for the implementation of high-strength steels, as many are available in coil form. The system has the potential to simplify the fabrication process, as the metal building industry has already demonstrated that these systems can be fabricated directly from steel coils with minimal human supervision required. The paired system also lends itself to a modular system with pre-installed sandwich panels or CLT panels.

1.1 Research Objectives

The goal of this project is to determine if a composite floor system framed with cold-rolled Z-sections can provide a competitive alternative to a comparable system framed with traditional W-shapes. The project will target the following objectives

Develop stiffened Z-shaped cross sections comparable to W14X22, W16X26-31, W18X35-40, W21x44-50 and W24x55-62 standard shapes

1.2 Scope and Significance

This research project has the potential to pave the way for a groundbreaking methodology in steel construction. By exploring the use of heavier gauge cold-formed steel, we aim to unlock opportunities for creating optimized shapes and cross sections, which could revolutionize the industry. Additionally, the adoption of higher strength steels could further enhance the competitiveness of steel construction.

1.3 Research Questions or Hypotheses

Can a composite floor system framed with cold-rolled Z-sections provide a competitive alternative to a comparable system framed with traditional W-shapes?

2. Overview of Previous Research

Seek and Avci (2024) developed a process utilizing the Direct Strength Method to predict the local buckling and distortional buckling strength of purlins with paired torsion bracing. In this paper, they have reformulated the methodology to account for the effect of slope in the structural behavior of the roof systems. The methodology utilizes the component stiffness method to calculate the anchorage forces within the purlin system and incorporates the effects of first-order and approximate second-order torsion for the prediction of stress distributions along purlin cross sections. The research showed that by properly accounting for the various biaxial bending and torsional moments and correctly quantifying the brace forces, the complex behavior of the Z-section could be accurately predicted, allowing for optimized performance of the members.

Seek, M. W., Avci, O. (2024). "Assessment of Purlins with Paired Torsion Bracing using Direct Strength Method: Sloped Roof Systems." Structures. Accepted March 5, 2024

2.1 Key Findings from Literature

- Paired torsion bracing is commonly used in purlin roof systems to support standing seam sheathing.
- The bracing is intended for torsion only and does not provide lateral restraint to the purlins. - This system eliminates the need for external anchoring as the sheathing provides the entire lateral restraint.

- Torsion braces are typically used between two adjacent purlins, and the torsion-only bracing configuration is achieved when the torsion braces are applied in an alternating arrangement.
- The component stiffness method is used for the assessment of interacting forces between the purlins, external braces, and sheathing, and is expanded to estimate geometric 2nd-order effects for the development of strength prediction methodology.
- The true stress distribution throughout the purlin cross sections is determined by taking the interaction between the braces, sheathing, and purlins into consideration, including torsion and biaxial bending effects in the calculations of the true stress distributions along the purlins.

2.2 Gaps in Knowledge

The research findings indicate that highly effective structural systems can be developed through the integration of paired purlins and the bracing between them. The proposed system employs paired Z-sections arranged back-to-back, supplemented by an X-brace diaphragm positioned at approximately the third points of the members. However, it was unclear whether the Z-shape would offer competitive advantages concerning both capacity and weight.

3. Development of Z-sections

For this research initiative, we are utilizing an analytical approach that commences with the geometric design of the Z-sections. Throughout the design phase, our focus is on ensuring that the moment of inertia and section modulus of the Z-sections are comparable to those of the lightest W-shapes available in each depth class for members commonly used in composite floor systems (ie, W14 through W21).

To facilitate this evaluation, the development of the cross sections adhered to the following philosophy. The bottom flange would be larger than the top flange to improve behavior of the composite section. The depth of each section was held to the nearest inch and for each given depth, the same cross-sectional dimensions were maintained and only the thickness of the material changed. The length of the flat plate needed to form the cross section targeted even two-inch increments.

Our primary objective is to develop Z-sections that have comparable wight and moment of inertia to existing W-shapes to compare the difference in behavior. To develop the cross section, the minimum bend radius for Hollow Structural Sections (HSS) (1.5 x thickness) was used. The detailed values for the moment of inertia and the section modulus for each Z-Section are provided in the table below. We have adopted the following naming convention. For example, the 14ZS4.5/7x0.1875 has an out-to-out depth of 14 in., a top flange width of 4.5 in, a bottom flange width of 7 in. and a thickness of 0.1875 in. The flange dimensions are measured from the web to the center of the stiffener bend. For each section a total stiffener length of 2 in. was used. An extensive list of cross section properties including location of centroid, shear center, plastic section properties, and torsion properties is provided in Appendix A for both the Z-sections and their comparable W-shape.

Table 1: Moment of inertia and section modulus comparation.

	MOMENT OF INERTIA			SECTION MODULUS		Area	
BEAM TYPE	Iz	Iy	PERCENTAGE OF I DIFF	Szt	Szb	AREA in^2	PERCENTAGE OF AREA DIFF
14ZS4.5/7x0.1875	163.92	52.57	-17.6%	21.55	25.63	5.35	-17.5%
W14X22	199.00	7.00		29.10	29.10	6.49	
16ZS4.5/7x0.25	291.94	68.54	-3.0%	33.75	39.73	7.56	-1.6%
W16X26	301.00	9.59		38.34	38.34	7.68	
16ZS4.5/7x0.3125	356.77	83.51	-4.9%	41.22	48.58	9.35	2.4%
W16X31	375.00	12.40		47.17	47.17	9.13	
18ZS5.5/8x0.3125	521.11	122.39	2.2%	53.99	62.42	10.60	2.9%
W18X35	510.00	15.30		57.63	57.63	10.30	
18ZS5.5/8x0.375	612.93	143.56	-0.1%	63.48	73.46	12.60	6.9%
W18x40	613.32	19.14		68.53	68.53	11.78	
21ZS4.5/7x0.375	803.05	98.31	-4.7%	71.41	82.32	12.97	-0.2%
W21X44	843.00	20.70		81.45	81.45	13.00	
21ZS4.5/7x0.4375	918.49	111.80	-6.7%	81.64	94.20	15.00	2.0%
W21X50	984.00	24.90		94.62	94.62	14.70	
24ZS6/8.5x0.375	1267.72	171.75	-6.1%	99.61	112.46	15.22	-6.0%
W24X55	1350.00	29.10		114.41	114.41	16.20	
24ZS6/8.5x0.4375	1454.50	196.09	-6.2%	114.25	129.07	17.62	-3.2%
W24X62	1550.00	34.50		130.80	130.80	18.20	

3.1 Composite properties

To facilitate the analysis of composite properties and enable a comprehensive comparison between W-shapes and Z-shapes, we have developed a specialized spreadsheet. Initially, we included the AISC shapes properties table, which contains relevant information about W-shapes. Following this, we created a data table for Z-shapes to allow for a direct and effective comparison of both cross-sectional profiles.

The spreadsheet is designed to present a side-by-side comparison of the W-Shape (indicated by a blue top ribbon) and the Z-Shape (indicated by a green top ribbon) see Figure 3. In the spreadsheet, the user can specify the beam cross section, beam span and spacing, as well as the depth of the deck and concrete cover over the deck. The spreadsheet calculates the moment of inertia and plastic moment strength of the fully composite cross section. Strength checks are provided for 3 states: 1) steel self-weight and construction load prior to concrete placement, 2) self-weight and construction load during concrete, and 3) occupancy loading. For the limit states during construction, the strength of the Z-section is based on the yield moment while the W-shape is evaluated at the plastic moment. With more detailed analysis, it is expected that the Z-section can resist moments that exceed the yield moment during construction.

An evaluation of vibration characteristics is provided according to the calculation method provided in AISC Design Guide 11. The spreadsheet calculates the partial composite strength of the system based on a percent composite value specified by the user. Users input their values into the yellow cells and choose options from the dropdown menus in the blue cells, while results will be displayed in the green cells. Additionally, the orange cells provide a clear pass or fail evaluation based on the results obtained.

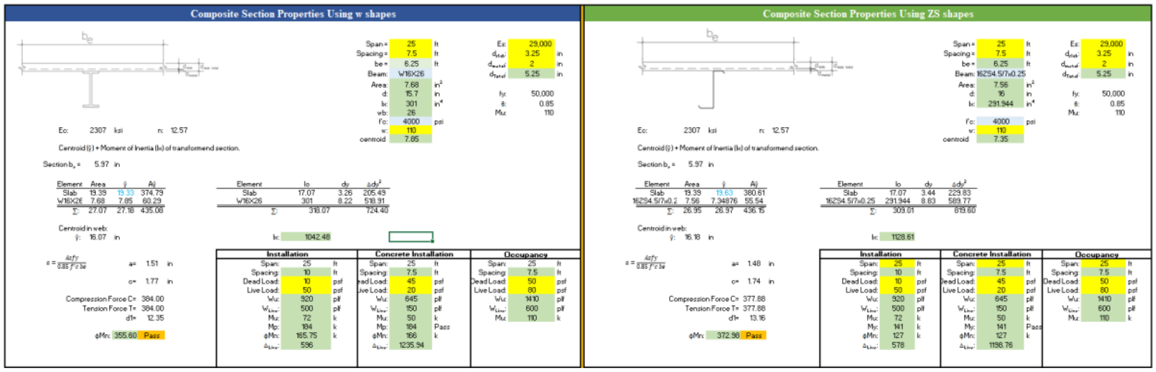

Figure 3: Side by Side View

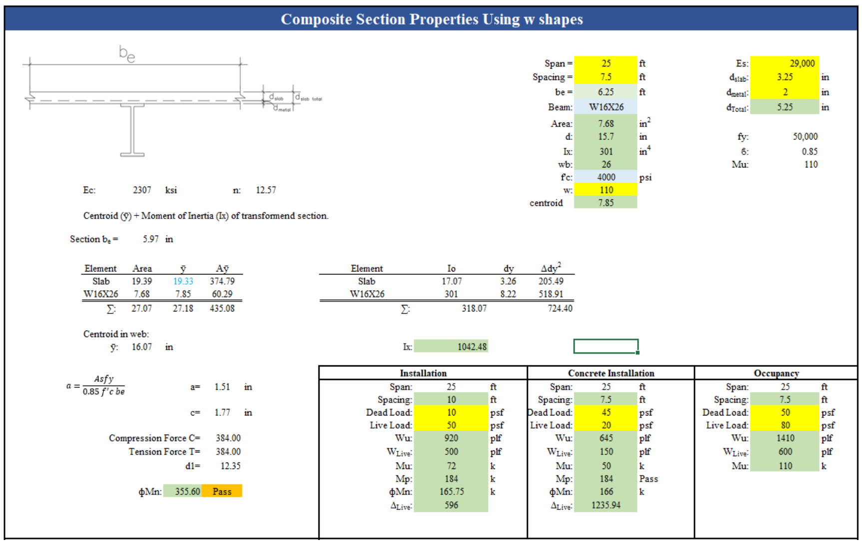

Figure 4: W-Shape composite calculation

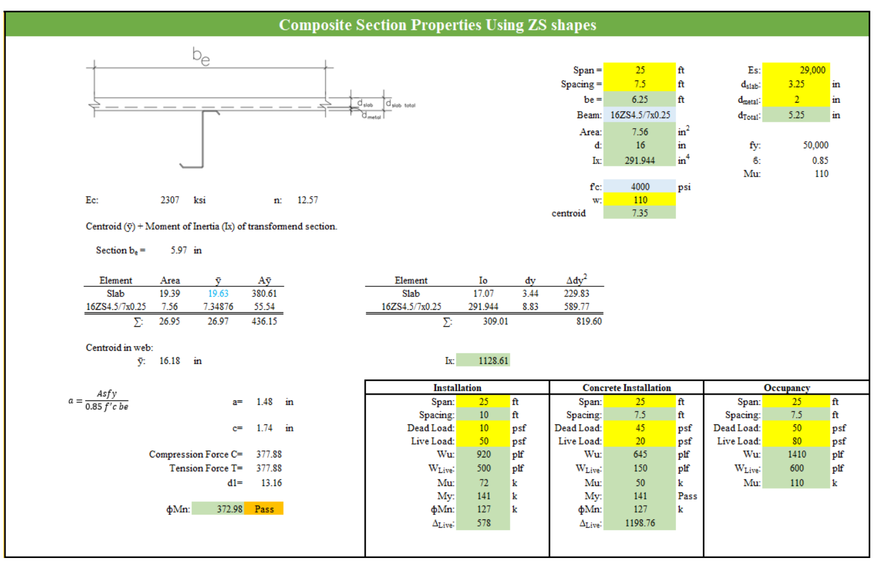

Figure 5: Z-Shape Composite calculation

To illustrate the elements of the calculator, a representative bay of a floor system is analyzed. A framing system for a typical exterior bay, as shown in Figure 6, will be evaluated for composite and partial composite using W-shapes and Z-shapes. The floor system is to be designed for an occupancy live load of 80 psf. Lightweight concrete with a unit weight of 110 pcf is used.

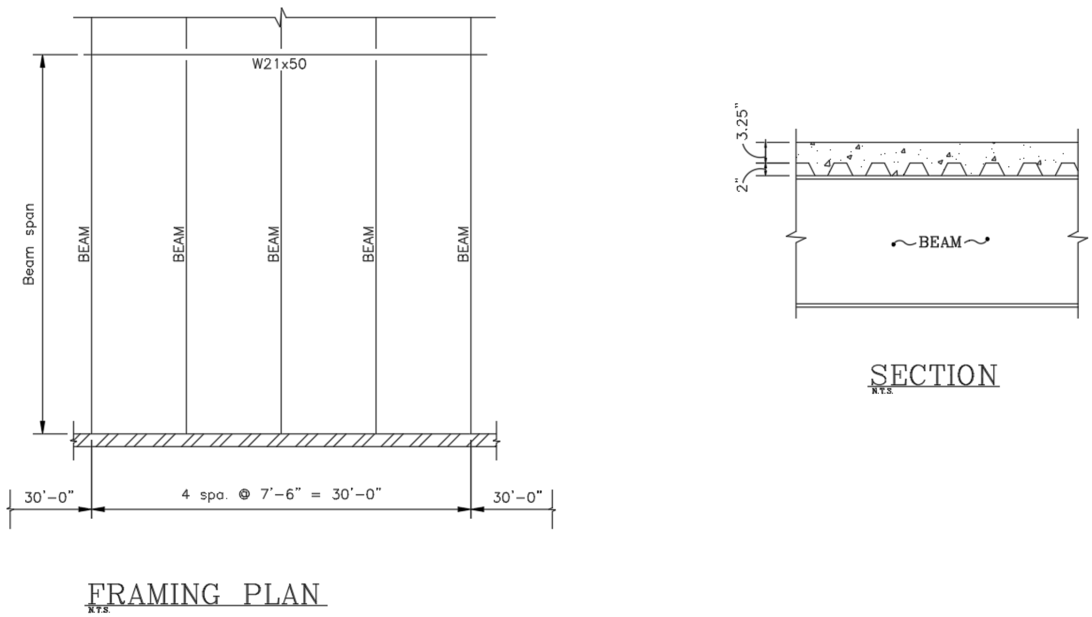

Figure 6: Layout of exterior bay

Properties are as follows for W16x26:

Span =	30	ft
Spacing =	7.5	ft
be =	7.5	ft
Beam:	W16X26	
Area:	7.68	in^2
d:	15.7	in
Ix:	301	in^4
wb:	26	
f'c:	4000	psi
w:	110	
centroid	7.85	

Es:	29,000	
d_{slab}:	3.25	in
d_{metal}:	2	in
d_{Total}:	5.25	in
fy:	50,000	
ϕ:	0.85	
Mu:	159	

Figure 7: W16x26 properties

Properties are as follows for 16ZS4.5/7x0.25:

Span =	30	ft	Es:	29,000	
Spacing =	7.5	ft	d_{slab}:	3.25	in
be =	7.5	ft	d_{metal}:	2	in
Beam:	16ZS4.5/7x0.25		d_{Total}:	5.25	in
Area:	7.56	in^2			
d:	16	in	fy:	50,000	
Ix:	292	in^4	б:	0.85	
wb	25.8	lb	Mu:	159	
f'c:	4000	psi			
w:	110				
centroid	7.35				

Figure 8: 16ZS4.5/7x0.25 properties

W-shape is evaluated based on plastic moment strength of the bare steel section. For the Z-section, we are conservatively using the yield moment. It is expected that the Z-sections have capacity above their yield moment but more detailed analysis is required.

It is essential to recognize the centroid of the Z-section is lower than that of the comparable W-shape, which results in an increased composite moment of inertia. In this example, the fully composite moment of inertia of the W16x26 is 1081.84 in^4 while the moment of inertia of the 16ZS4.5/7x0.25 is 1172.21 in^4, which represents a nearly 10% increase. Additionally, the plastic design moment for the W16x26 is 359.21 kip-ft while the design strength of the 16ZS4.5/7x0.25 is 5% higher at 376.48 kip-ft.

Using the same slab configuration (2" deck with 3.25" cover) and beam spacing of 7'-6" (assuming the full width of the slab is effective), the fully composite design moment strength and moment of inertia for each Z-section and W-shape are shown in Tables 5 respectively. The comparison shows typically a slight increase in both the design moment strength and moment of inertia.

In order to ensure stability during the construction process, the moment strength is evaluated for two conditions. The first condition is during the installation of the steel members, prior to the placing concrete. During this phase, it is assumed that there will be a dead load of 10 psf and a live load of 50 psf, resulting in a required moment strength of 78 k-ft. The second phase takes place during the placement of the concrete. In this phase, the applied dead load increases to 42 psf, while the live load is reduced to 20 psf. For the given loading conditions, the required moment strength is adjusted to 70 k-ft. These required moments are compared to the design strength of the bare steel section. For the W16x26, the full plastic moment strength (166 kip-ft) is used and provides much greater strength than required. For the Z-shape, the design yield moment (127 kip-ft) is conservatively used. It is anticipated that the capacity of the bare Z-section will exceed the yield moment however more detailed analysis is required.

For analyzing the strength during service, the composite strength of the system is used. For this example, the required moment strength for the occupancy load case is 159 kip-ft. The fully composite strength of both the W-shape and Z-section, 359 kip-ft and 376 kip-ft respectively, is much greater than what is required. Therefore, to produce a more efficient design, it is desirable to design the composite floor as partially composite.

To simplify the calculation of the partially composite properties for the Z-section, the geometry of the Z was subdivided into simplified areas in the same way that the cross section of a W-shape is simplified. Figure 9(a) depicts the geometry distribution of a Z section, whereas Figure 7(b) illustrates the geometry distribution of a W section. Similar to the way that the fillet of the W-shape is approximated as a rectangular area, for the Z-shape, the flange stiffener and the two bend radii adjacent to the flange are lumped into an area and distributed evenly over the projected height of the stiffener. Additionally, Table 2 presents a comprehensive analysis of the cross-sectional geometry for all Z shapes.

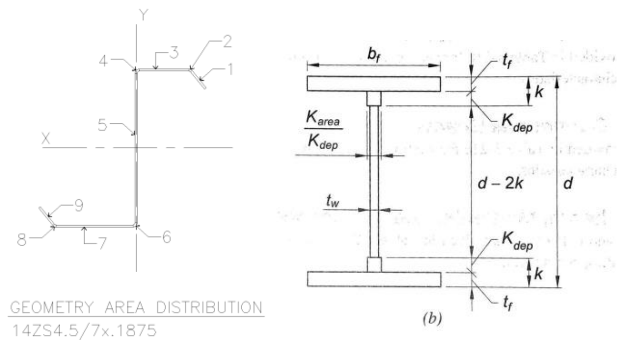

Figure 9: Geometry distribution for Z-shapes and W-shapes

Table 2: cross section geometry

	Cross Section Geometry																
BEAM TYPE	1	2	3	4	5	6	7	8	9	t	$D_{tflange}$	$D_{bflange}$	D_{web}	A_{fillet}	$A_{tflange}$	$A_{bflange}$	A_{web}
14ZS4.5/7x0.1875	0.334	0.0609	0.7149	0.1076	2.4492	0.1076	1.1836	0.0609	0.334	0.1875	1.6526	1.4651	10.69	0.77721	0.7149	1.1836	2.01
16ZS4.5/7x0.25	0.4271	0.1082	0.8959	0.1913	3.6875	0.1913	1.5209	0.1082	0.4271	0.25	1.6928	1.4428	12.61	1.0873	0.8959	1.5209	3.15
16ZS4.5/7x0.3125	0.5112	0.1691	1.0483	0.299	4.5117	0.299	1.8295	0.1691	0.5112	0.3125	1.733	1.4205	12.53	1.42321	1.0483	1.8295	3.92
18ZS5.5/8x0.3125	0.5861	0.2435	1.547	0.4305	6.0469	0.4305	2.4845	0.2435	0.5861	0.3125	1.7731	1.4606	14.45	1.71654	1.547	2.4845	4.52
18ZS5.5/8x0.375	0.5861	0.2435	1.547	0.4305	6.0469	0.4305	2.4845	0.2435	0.5861	0.375	1.7731	1.3981	14.45	1.78439	1.547	2.4845	5.42
21ZS4.5/7x0.375	0.5861	0.2435	1.172	0.4305	7.1719	0.4305	2.1095	0.2435	0.5861	0.375	1.7731	1.3981	17.45	1.78439	1.172	2.1095	6.55
21ZS4.5/7x0.4375	0.6965	0.2486	1.4074	0.4395	8.4219	0.4395	2.5012	0.2486	0.6965	0.4375	1.8133	1.3758	17.37	1.98651	1.4074	2.5012	7.60
24ZS6/8.5x0.375	0.5861	0.2435	1.7345	0.4305	8.2969	0.4305	2.672	0.2435	0.5861	0.375	1.7731	1.3981	20.45	1.78439	1.7345	2.672	7.67
24ZS6/8.5x0.4375	0.6519	0.3314	1.9233	0.586	9.543	0.586	3.0171	0.3314	0.6519	0.4375	1.8133	1.3758	20.37	2.17121	1.9233	3.0171	8.91

Once the geometry was established, we proceeded to calculate the location of the plastic neutral axis, which is essential for determining partially composite moment strength. The calculations are performed systematically for the user, with the only required input being the desired percentage of fully composite. As shown in Figure 10, the nominal moment strength, Mn, value for the 16ZS4.5/7x0.2 shape at 15% composite is 188.82, whereas the W-shape exhibits a value of 194.77. The decrease in moment strength is a function of the redistribution of the area on the Z shape, this generates a conservative approximation.

Partial Composite Section Properties Using w shapes

C_{steel} =	384	Cmax=	384		
C_{slab} =	994.5				
Percentage Of Composite	15%				
Q_N =	57.6	tf=	0.345	tw=	0.250
a =	0.19	k=	0.747	t=	13.625
		$A_{bflange}$=	1.8975		
Aflange=	1.8975	$A_{tflange}$=	1.8975		
A_{WEB}=	3.55	$b_{tflange}$=	5.5		
A_{FILLET}=	0.167				
K_{dep}=	0.402				
T_{dep}=	0.415				
A_{ST} =	4.416				
A_{sc} =	3.264				
hpna=	10.15				
Mn=	194.77				
ϕMn:	175.29				

Partial Composite Section Properties Using ZS shapes

C_{steel} =	377.884	Cmax=	377.884		
C_{slab} =	994.5				
Percentage Of Composite	15%				
Q_N =	56.6826	tf=	0.25	tw=	0.25
a =	0.19	k=	1.532089	T=	12.93582223
		$A_{bflange}$=	1.5209		
Aflange=	0.90	$A_{tflange}$=	0.8959		
A_{WEB}=	3.23	$b_{tflange}$=	3.5836		
A_{FILLET}=	0.95				
K_{dep}=	1.28				
T_{dep}=	0.74				
A_{ST} =	4.35				
A_{sc} =	3.21				
hpna=	9.02				
Mn=	188.82				
ϕMn:	169.94				

Figure 10: Partial composite sections for W-shapes and Z-shapes

3.2 Vibration Analysis

A dedicated portion of the calculator is designed to assess the vibration response of the composite floor system due to walking excitations. In accordance with the standards outlined in the AISC Design Guide 11, this analysis utilizes the walking excitation criterion, which is defined as low-frequency vibrations occurring at frequencies below 9 Hz. This methodology enables a comprehensive evaluation of how typical activities, such as walking or running, influence both the structural integrity and the comfort of occupants. By approximating the response of the floor to these vibrational effects, we can ensure that the design adheres to established performance standards and provides a serviceable environment for the occupants.

The vibration evaluation process commences with a detailed analysis of the beams. This involves calculating the transformed moment of inertia, which indicates how the beam will resist bending under load. Next, the mid-span deflection is assessed, measuring how much the beam deflects at its center when subjected to a load. Finally, the beam panel mode frequency, expressed in hertz (Hz), is determined to identify the natural frequency at which the beam vibrates. We will perform similar calculations for the girder designated as a W21x50, with a span measuring 30 feet.

Following this, we will assess the combined panel mode to verify that the peak acceleration is below the tolerance limit established in Table 3 (Table 4.1 of the AISC Design Guide 11).

Table 3: Recommended Acceleration limits for floors (from AISC DG11)

Recommended Tolerance Limits for Building Floors	
Occupancy	Acceleration Limit $a_o/g \times 100\%$
Offices, residences, churches, schools and quiet areas	0.50%
Shopping malls	1.50%

The results of this analysis are shown in Figure 11 for the W-shape and Figure 12 for the Z-section. Both of the systems satisfy the acceleration limit of 0.50%, with the Z-section showing a slightly improved performance. Because the Z-section has a larger composite moment of inertia, the frequency of the panel is slightly increased and more weight in the panel mode is activated, which results in the slightly lower acceleration of the Z-section floor system. Ultimately, the vibration serviceability criteria controls the design of this floor system.

Vibration Of Steel-Framed Structural System for W- Shape

Ec=	2,307.38		Asummed Loads								
Deck Selfweight=	2.00	psf	Dead Load:	4	psf						
Slab+deck weight=	40.96		Live Load:	11	psf						
n =	9.31										
min[0.4L_j, S]=	90.00	in	Girder:	W21X50		Girder Length:	30	ft	w:	50	
Transformed Conc. Slab Area =	31.42		d:	20.80		Area:	14.7		Ix:	984	
$\bar{y}$:	9.22	in	$\bar{y}$:	10.96	in						
I_j=	1,141.28	in^4	I_g=	3,274.42	in^4						
w_j=	445.69	plf	w_g=	1,832.75	plf	Evaluation					
Δ_j=	0.25	in	Δ_g=	0.35	in	fn=	4.58	Hz			
f_j=	7.14	Hz	f_g=	5.96	Hz	Δ'_g=	0.36				
D_s=	8.25	in^4/ft	D_j=	152.17	in^4/ft	W=	95,418.50				
D_j=	152.17	in^4/ft	D_g=	109.15	in^4/ft	Acceleration limit:	0.46%				
B_j=	28.95	ft	B_g=	58.68	ft		PASS				
W_j=	77,411.50	lb	W_g=	107,541.59	lb						

Figure 11: Vibration for W-shape

Vibration Of Steel-Framed Structural System for Z- Shape

Ec=	2307		Asummed Loads								
Deck Selfweight=	2	psf	Dead Load:	4	psf						
Slab+deck weight=	40.96		Live Load:	11	psf						
n =	9.31										
min[0.4L_j, S]=	90.00	in	Girder:	W21X50		Girder L	30	ft	w:	50	
Transformed Conc. Slab Area =	31.42		d:	20.80		Area:	14.7		Ix:	984	
$\bar{y}$:	9.90	in	$\bar{y}$:	10.96	in						
I_j=	1,237.73	in^4	I_g=	3,274.42	in^4						
w_j=	445.46	plf	w_g=	1,831.84	plf	Evaluation					
Δ_j=	0.23	in	Δ_g=	0.35	in	fn=	4.65	Hz			
f_j=	7.44	Hz	f_g=	5.96	Hz	Δ'_g=	0.37				
D_s=	8.25	in^4/ft	D_j=	165.03	in^4/ft	W=	96,878.97				
D_j=	165.03	in^4/ft	D_g=	109.15	in^4/ft	Acceleration limit	0.44%				
B_j=	28.37	ft	B_g=	59.88	ft		PASS				
W_j=	75,818.42	lb	W_g=	109,690.30	lb						

Figure 12: Vibration for Z-shape

3.3 Limitations and Assumptions

The current research does not consider the strength of the studs transferring the transverse shear between the steel section and concrete slab. There are limitations on the thickness of the base metal relative to the diameter of the stud which may not be satisfied for larger diameter studs paired with thinner Z-sections. The analysis of the Z-sections assumes that the Z-sections have a fully constrained stress distribution. Because the Z-sections have a rotated principal axes, they are subject to lateral bending effects and depending to the extent of the restraint provided by the braces relative to the slab/deck the stresses may deviate from a constrained bending stress distribution which could impact the strength of the Z-section. Analysis assumes that the Z-sections are fully effective, and local buckling does not control the strength or reduce the moment of inertia.

4. Conclusion

We have successfully developed an analytical tool specifically designed for evaluating the performance of the proposed Z-sections relative to that of comparable W-shapes in composite floor systems.

The Z-sections developed provide improved composite performance relative to the W-shape. The fully composite moment of inertia and design moment strength of the Z-section are greater than that of the comparable W-shape when considering the relative difference in the cross- sectional area. Table 5 provides a side-by-side comparison of the fully composite moment of inertia and design moment strength for each type. Table 5 should be considered in conjunction with Table 1. In all cases the percent difference in strength between sections exceeds the percent difference in cross sectional area. The increase in composite capacity for the Z-section is a result of the larger bottom flange which shifts the elastic and plastic neutral axes. The increase in moment of inertia helps to improve vibration performance, which often controls the design of composite floor systems.

Using the tool there is compelling evidence that Z-section beams could be a viable alternative to W-shapes in composite floor systems. As a result of an unsymmetric section with a larger bottom flange, the Z-sections exhibit slight increases in composite strength and vibration performance. As a result of the single bottom flange, the Z-section allows for a direct drop in connection to girders.

However, it would take a significant investment tooling to create these Z-sections and to utilize them would represent a substantial change in the way that the industry has utilized steel in composite floor systems for decades. It is not clear whether the advantages that the Z-sections provide over W-shapes are substantial enough to overcome the momentum that the industry has in using W-shapes in composite floor systems. However, there may be other applications such as panelized floor systems or residential systems that may have shorter spans and lower required loads where a rolled Z-section may provide advantageous performance over a conventional steel or concrete system. Additional research is also required to better understand the local and distortional buckling behavior of these thin-walled sections and how their interaction with different floor systems can affect their strength and behavior.

Table 4: W-shape and Z-shape comparation of fully composite

Comparison of Fully Composite Properties				
BEAM TYPE	**Ix**	**% Increase for Ix**	**φMn**	**% Increase for φMn**
14ZS4.5/7x0.1875	733.21	-6%	249.25	-11%
W14X22	776.32		281.58	
16ZS4.5/7x0.25	1172.21	8%	376.48	5%
W16X26	1081.84		359.21	
16ZS4.5/7x0.3125	1383.04	9%	460.68	8%
W16X31	1274.06		426.40	
18ZS5.5/8x0.3125	1825.23	11%	557.82	9%
W18X35	1641.65		512.11	
18ZS5.5/8x0.375	2075.09	11%	655.59	12%
W18x40	1870.64		585.69	
21ZS4.5/7x0.375	2664.47	7%	750.94	6%
W21X44	2492.46		708.72	
21ZS4.5/7x0.4375	2956.88	6%	859.02	8%
W21X50	2776.63		796.50	
24ZS6/8.5x0.375	3749.18	3%	955.29	-0.01%
W24X55	3643.04		955.38	
24ZS6/8.5x0.4375	4157.86	4%	1093.10	3%
W24X62	4016.26		1065.59	

4.1 Key Finding

The results obtained from the composite calculator demonstrate that we have successfully developed Z-shaped geometries with strength characteristics closely aligned with those of W-shaped geometries. This finding is significant as it establishes a foundation for advancing further research on the application of cold-formed steel.

4.2 Implications of the Research

This research endeavor aims to establish the foundational stage of a more comprehensive investigation focused on the comparative analysis of Z and W shapes. By methodically assessing their geometrical properties and structural performance, this study seeks to offer valuable insights into the potential applications of cold-formed steel. The objective is to facilitate innovative approaches to utilizing cold-formed steel, thereby expanding its applicability in construction and manufacturing processes.

4.3 Potential Applications

The primary objective of this study is to investigate the potential substitution of W-shaped hot-rolled steel beams with Z-shaped rolled steel beams within construction applications. This transition may facilitate significant cost reductions for small-scale construction projects, which constitute a considerable majority of construction activities.

By implementing Z-shaped beams, organizations can realize savings in several key areas:

1. Manufacturing Costs: The design of Z-shaped beams allows for more efficient production processes, potentially resulting in decreased material usage and reduced energy consumption during fabrication when compared to W-shaped beams.

2. Handling and Transportation: The unique geometry of Z-shaped beams can streamline handling and storage operations, leading to lower transportation and on-site management expenses.

3. Storage Efficiency: The compact design of Z-shaped beams may optimize storage capabilities, promoting more effective utilization of space at construction sites and in warehouses.

In addition to cost considerations, it is essential to evaluate the environmental implications associated with these materials. The production processes for W-shaped beams are associated with higher carbon emissions in comparison to those involved in the manufacture of cold-formed steel, which includes Z-shaped configurations. This shift towards Z-shaped beams not only contributes to cost savings but also aligns with the increasing emphasis on sustainable construction practices. Overall, the adoption of Z-shaped beams presents both economic advantages and positive ecological outcomes for the construction industry.

4.4 Contributions to the Field

This research contributes to the field of Civil Engineering by laying the groundwork for the future development of applications involving cold-formed structural steel. It emphasizes the material's potential in construction and engineering. By analyzing its properties, benefits, and opportunities for innovation, this study aims to provide insights into the effective utilization of cold-formed steel in modern construction practices.

4.5 Lessons Learned

During the research process, we encountered several trials and errors while reconfiguring the shapes in order to identify the most effective configuration. This process is inherently lengthy and requires meticulous attention to detail. Each adjustment demands a high degree of precision to ensure that we progressively move closer to the optimal outcome. Despite the inherent challenges associated with this rigorous approach, it is essential for achieving accurate and reliable results.

4.6 Recommendations for Further Research

Future research efforts should aim to explore a variety of alternative Z-shaped configurations to assess their potential for improving the overall strength of the beam. This could involve experimenting with larger top or bottom flanges, as these structural modifications may contribute to increased load-bearing capacity. Additionally, it would be valuable to investigate whether adjusting the 90-degree angles on the lips of the Z-shape affects the strength and performance characteristics of the beam.

References

Michael W. Seek , Onur Avci (2022) "Evaluation of local and distortional buckling strength of purlins with paired torsion bracing using Direct Strength Method" *Journal of constructional steel research* V 203. April 2023 https://www.sciencedirect.com/science/article/abs/pii/S0143974X22005685

Structural Steel Construction Manual (16th Edition) American Institute of Steel Construction 2023 ISBN 978-1-56424-116-0

Steel Design Guide 11, Vibration of Steel-Framed Structural Systems Due to Human Activity (Second Edition) American Institute of Steel Construction 2016

5.1 Data Collection Instruments

Structural Steel Construction Manual (16th Edition) American Institute of Steel Construction 2023 ISBN 978-1-56424-116-0

Software, Structural Analysis and Design, SkyCiv Engineering

Z-Shape Calculator Spreadsheet developed by Israel Barreto and Dr. Michael Seek

Supplementary Figures and Tables

14ZS4.5/7x0.1875		
Thickness	0.1875	in
Height	14	in
Top Flange	4.5	in
Bottom Flange	7	in
Lips	2	in
Lips Angle	50	deg
Internal Radius	0.2813	in
External Radius	0.375	in
Length	30	in

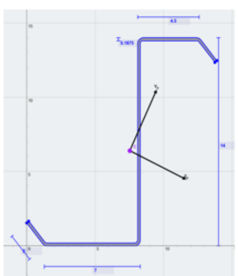

Geometric Properties		
Area	5.35276	in2
Centroidz	7.53121	in
Centroidy	6.39521	in
Moment of Inertia		
Iz	163.919	in4
Iy	52.5671	in4
Izy	68.3991	in4
Izp	196.438	in4
Iyp	20.0487	in4
α	25.4274	°
rz	5.53384	in
ry	3.13378	in
rzp	6.05792	in
ryp	1.93533	in
Section Moduli		
Szt	21.5547	in3
Szb	25.6316	in3
Syt	8.2751	in3
Syb	6.9799	in3
Zzp	29.152	in3
Zyp	8.7623	in3
PNAz	0.643379	in
PNAy	−0.645208	in
PNAzp	61.6154 x10 -3	in
PNAyp	−0.299047	in
Shear Properties		
Az	1.90493	in2
Ay	2.43025	in2
SCz	0.135719	in
SCy	3.07539	in
Qz	13.6284	in3
Qy	6.08221	in3
Torsion and Warping Properties		
J	[illegible]	in4
r	0.210725	in
Iw	1390.14	in6
βz, pos	−6.72914	in
βy, pos	−0.805735	in
βzp, pos	−5.9836	in
βyp, pos	6.97688	in
Section Capacity		
Ry,base	36	ksi
Mpl,zp	87.456	kip-ft
Mpl,yp	26.2869	kip-ft
Mpl,z	81.5361	kip-ft
Mpl,y	32.5218	kip-ft
Npl,x	192.699	kip

W14X22

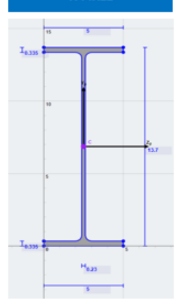

Geometric Properties		
Area	6.49	in2
Centroidz	2.5	in
Centroidy	6.85	in
Moment of Inertia		
Iz	199	in4
Iy	7	in4
Izy	0	in4
rz	5.52353	in
ry	1.03798	in
Section Moduli		
Szt	29.0511	in3
Szb	29.0511	in3
Syt	2.8	in3
Syb	2.8	in3
Zzp	33.2	in3
Zyp	4.39	in3
PNAz	0	in
PNAy	0	in
Shear Properties		
Az	3.02241	in2
Ay	3.05471	in2
Apl,z	3.35	in2
Apl,y	3.07395	in2
SCz	4.9315 x10 -6	in
SCy	0	in
Qz	16.5565	in3
Qy	2.19562	in3
Torsion and Warping Properties		
J	0.208	in4
r	0.557317	in
Iw	314	in6
βz, pos	0	in
βy, pos	-9.86301 x10 -6	in
Section Capacity		
Ry,base	36	ksi
Mpl,z	99.339	kip-ft
Mpl,y	13.1736	kip-ft
Vpl,z	69.5862	kip
Vpl,y	63.8521	kip
Npl,x	233.894	kip

16ZS4.5/7x0.25		
Thickness	0.25	in
Height	16	in
Top Flange	4.5	in
Bottom Flange	7	in
Lips	2	in
Lips Angle	50	deg
Internal Radius	0.375	in
External Radius	0.5	in
Length	30	in

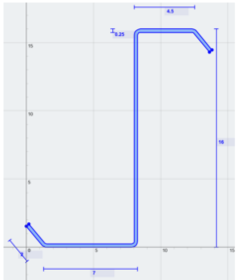

Geometric Properties

Area	7.558	in2
Centroidz	7.542	in
Centroidy	7.349	in

Moment of Inertia

Iz	291.9	in4
Iy	68.54	in4
Izy	103.1	in4
Izp	332.2	in4
Iyp	28.26	in4
α	21.35	˚
rz	6.215	in
ry	3.011	in
rzp	6.63	in
ryp	1.934	in

Section Moduli

Szt	33.75	in3
Szb	39.73	in3
Syt	10.92	in3
Syb	9.087	in3
Zzp	45.07	in3
Zyp	12.27	in3
PNAz	0.598	in
PNAy	-0.599	in
PNAzp	1x10 -3	in
PNAyp	-0.333	in

Shear Properties

Az	2.447	in2
Ay	3.668	in2
SCz	0.139	in
SCy	3.568	in
Qz	21.49	in3
Qy	8.063	in3

Torsion and Warping Properties

J	0.157	in4
r	0.281	in
Iw	2388	in6
βz, pos	-7.755	in
βy, pos	-0.948	in
βzp, pos	-7.162	in
βyp, pos	7.44	in

Section Capacity

Ry,base	36	ksi
Mpl,zp	135.2	kip-ft
Mpl,yp	36.82	kip-ft
Mpl,z	128.7	kip-ft
Mpl,y	42.87	kip-ft
Npl,x	272.1	kip

W16X26

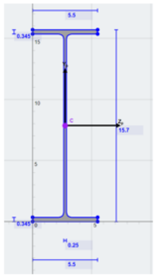

Geometric Properties

Area	7.68	in2
Centroidz	2.75	in
Centroidy	7.85	in

Moment of Inertia

Iz	301	in4
Iy	9.59	in4
Izy	0	in4
rz	6.2683	in
ry	1.11632	in

Section Moduli

Szt	38.3439	in3
Szb	38.3439	in3
Syt	3.48727	in3
Syb	3.48727	in3
Zzp	44.2	in3
Zyp	5.48	in3
PNAz	0	in
PNAy	0	in

Shear Properties

Az	3.40775	in2
Ay	3.79358	in2
Apl,z	3.795	in2
Apl,y	3.83875	in2
SCz	1.65742 x10 -6	in
SCy	-15.6477 x10 -6	in
Qz	22.1706	in3
Qy	2.74299	in3

Torsion and Warping Properties

J	0.262	in4
r	0.577266	in
Iw	565	in6
βz, pos	35.2953 x10 -6	in
βy, pos	-3.31484 x10 -6	in

Section Capacity

Ry,base	36	ksi
Mpl,z	133.024	kip-ft
Mpl,y	16.458	kip-ft
Vpl,z	78.8297	kip
Vpl,y	79.7385	kip
Npl,x	277.17	kip

16ZS4.5/7x0.3125		
Thickness	0.3125	in
Height	16	in
Top Flange	4.5	in
Bottom Flange	7	in
Lips	2	in
Lips Angle	50	deg
Internal Radius	0.4688	in
External Radius	0.625	in
Length	30	in

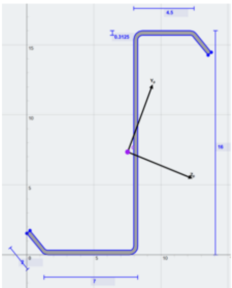

Geometric Properties

Area	9.348	in2
Centroidz	7.51	in
Centroidy	7.344	in

Moment of Inertia

Iz	356.8	in4
Iy	83.51	in4
Izy	126.1	in4
Izp	406	in4
Iyp	34.25	in4
α	21.35	˚
rz	6.178	in
ry	2.989	in
rzp	6.591	in
ryp	1.914	in

Section Moduli

Szt	41.22	in3
Szb	48.58	in3
Syt	13.37	in3
Syb	11.12	in3
Zzp	55.38	in3
Zyp	15.02	in3
PNAz	0.593	in
PNAy	-0.59	in
PNAzp	82.484	in
PNAyp	-0.33	in

Shear Properties

Az	3.031	in2
Ay	4.559	in2
SCz	0.144	in
SCy	3.583	in
Qz	26.41	in3
Qy	9.91	in3

Torsion and Warping Properties

J	0.303	in4
r	0.353	in
Iw	2863	in6
βz, pos	-7.79	in
βy, pos	-0.94	in
βzp, pos	-7.2	in
βyp, pos	7.481	in

Section Capacity

Ry,base	36	ksi
Mpl,zp	166.1	kip-ft
Mpl,yp	45.07	kip-ft
Mpl,z	158.1	kip-ft
Mpl,y	52.89	kip-ft
Npl,x	336.5	kip

W16X31

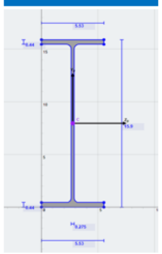

Geometric Properties

Area	9.13	in2
Centroidz	2.765	in
Centroidy	7.95	in

Moment of Inertia

Iz	375	in4
Iy	12.4	in4
Izy	0	in4
rz	6.4182	in
ry	1.1659	in

Section Moduli

Szt	47.17	in3
Szb	47.17	in3
Syt	4.4846	in3
Syb	4.4846	in3
Zzp	54	in3
Zyp	7.03	in3
PNAz	0	in
PNAy	0	in

Shear Properties

Az	4.3249	in2
Ay	4.2322	in2
Apl,z	4.8664	in2
Apl,y	4.2515	in2
SCz	0	in
SCy	0	in
Qz	27.126	in3
Qy	3.5235	in3

Torsion and Warping

J	0.461	in4
r	0.678	in
Iw	739	in6
βz, pos	1.34612 x10 -6	in
βy, pos	0	in

Section Capacity

Ry,base	36	ksi
Mpl,z	162.76	kip-ft
Mpl,y	21.141	kip-ft
Vpl,z	101.09	kip
Vpl,y	88.312	kip
Npl,x	329.35	kip

18ZS5.5/8x0.3125		
Thickness	0.3125	in
Height	18	in
Top Flange	5.5	in
Bottom Flange	8	in
Lips	2	in
Lips Angle	50	deg
Internal Radius	0.4688	in
External Radius	0.625	in
Length	34	in

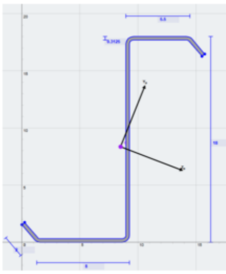

Geometric Properties

Area	10.6	in2
Centroidz	8.51	in
Centroidy	8.35	in

Moment of Inertia

Iz	521	in4
Iy	122	in4
Izy	186	in4
Izp	594	in4
Iyp	49.3	in4
α	21.5	˚
rz	7.01	in
ry	3.4	in
rzp	7.49	in
ryp	2.16	in

Section Moduli

Szt	54	in3
Szb	62.4	in3
Syt	16.9	in3
Syb	14.4	in3
Zzp	71.3	in3
Zyp	19.3	in3
PNAz	0.6	in
PNAy	-0.6	in
PNAzp	81.77 73	in
PNAyp	-0.3	in

Shear Properties

Az	3.56	in2
Ay	5.13	in2
SCz	0.16	in
SCy	3.57	in
Qz	34	in3
Qy	12.6	in3

Torsion and Warping Properties

J	0.34	in4
r	0.36	in
Iw	5519	in6
βz, pos	-7.8	in
βy, pos	-0.9	in
βzp, pos	-7.2	in
βyp, pos	7.59	in

Section Capacity

Ry,base	36	ksi
Mpl,zp	214	kip-ft
Mpl,yp	57.8	kip-ft
Mpl,z	204	kip-ft
Mpl,y	67.9	kip-ft
Npl,x	382	kip

W18x35

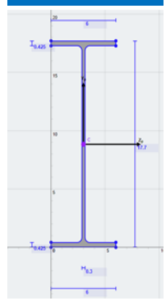

Geometric Properties

Area	10.3	in2
Centroidz	3	in
Centroidy	8.85	in

Moment of Inertia

Iz	510	in4
Iy	15.3	in4
Izy	0	in4
rz	7.03919	in
ry	1.2203	in

Section Moduli

Szt	57.6271	in3
Szb	57.6271	in3
Syt	5.1	in3
Syb	5.1	in3
Zzp	66.5	in3
Zyp	8.06	in3
PNAz	0	in
PNAy	0	in

Shear Properties

Az	4.53725	in2
Ay	5.11823	in2
Apl,z	5.1	in2
Apl,y	5.1825	in2
SCz	0	in
SCy	50.3653 x10 -6	in
Qz	33.3044	in3
Qy	4.03312	in3

Torsion and Warping Properties

J	0.506	in4
r	0.67712	in
Iw	1140	in6
βz, pos	-100.731 x10 -6	in
βy, pos	0	in

Section Capacity

Ry,base	37.7098	ksi
Mpl,z	209.317	kip-ft
Mpl,y	25.3479	kip-ft
Vpl,z	110.969	kip
Vpl,y	112.764	kip
Npl,x	388.663	kip

18ZS5.5/8x0.375		
Thickness	0.375	in
Height	18	in
Top Flange	5.5	in
Bottom Flange	8	in
Lips	2	in
Lips Angle	50	deg
Internal Radius	0.5625	in
External Radius	0.75	in
Length	34	in

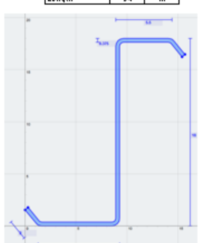

Geometric Properties

Area	12.599	in2
Centroidz	8.4777	in
Centroidy	8.3442	in

Moment of Inertia

Iz	612.93	in4
Iy	143.56	in4
Izy	218.53	in4
Izp	698.92	in4
Iyp	57.572	in4
α	21.479	˚
rz	6.975	in
ry	3.3756	in
rzp	7.4482	in
ryp	2.1377	in

Section Moduli

Szt	63.478	in3
Szb	73.456	in3
Syt	19.888	in3
Syb	16.934	in3
Zzp	84.282	in3
Zyp	22.688	in3
PNAz	0.5932	in
PNAy	-0.5942	in
PNAzp	81.0905 x10 -3	in
PNAyp	-0.3258	in

Shear Properties

Az	4.2385	in2
Ay	6.1226	in2
SCz	0.1617	in
SCy	3.5894	in
Qz	40.187	in3
Qy	14.866	in3

Torsion and Warping Properties

J	0.5874	in4
r	0.423	in
Iw	6383.6	in6
βz, pos	-7.8082	in
βy, pos	-0.9062	in
βzp, pos	-7.2198	in
βyp, pos	7.6344	in

Section Capacity

Ry,base	36	ksi
Mpl,zp	252.85	kip-ft
Mpl,yp	68.065	kip-ft
Mpl,z	240.72	kip-ft
Mpl,y	80.477	kip-ft
Npl,x	453.55	kip

W18x40

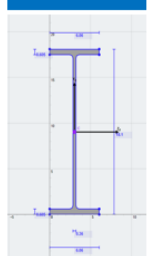

Geometric Properties

Area	11.7804	in2
Centroidz	3.01	in
Centroidy	8.95	in

Moment of Inertia

Iz	613.317	in4
Iy	19.1442	in4
Izy	0	in4
rz	7.21542	in
ry	1.27479	in

Section Moduli

Szt	68.527	in3
Szb	68.527	in3
Syt	6.36019	in3
Syb	6.36019	in3
Zzp	78.5361	in3
Zyp	9.9693	in3
PNAz	0	in
PNAy	0	in

Shear Properties

Az	5.57035	in2
Ay	5.44831	in2
Apl,z	4078.06	in2
Apl,y	3531.04	in2
SCz	-4.76315 x10 -6	in
SCy	-40.4099 x10 - 6	in
Qz	39.268	in3
Qy	4.98467	in3

Torsion and Warping

J	0.829599	in4
r	0.796205	in
Iw	1433.35	in6
βz, pos	80.8197 x10 -6	in
βy, pos	9.5263 x10 -6	in

Section Capacity

Ry,base	37.7098	ksi
Mpl,z	246.798	kip-ft
Mpl,y	31.3284	kip-ft
Vpl,z	88.7326 x103	kip
Vpl,y	76.8304 x103	kip
Npl,x	444.238	kip

21ZS4.5/7x0.375		
Thickness	0.375	in
Height	21	in
Top Flange	4.5	in
Bottom Flange	7	in
Lips	2	in
Lips Angle	50	deg
Internal Radius	0.5625	in
External Radius	0.75	in
Length	36	in

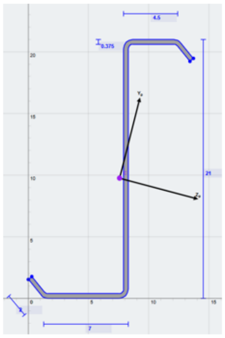

Geometric		
Area	12.9735	in2
Centroidz	7.56785	in
Centroidy	9.75479	in
Moment of Inertia		
Iz	803.047	in4
Iy	98.3115	in4
Izy	198.342	in4
Izp	855.033	in4
Iyp	46.3248	in4
α	14.6872	°
rz	7.86758	in
ry	2.75279	in
rzp	8.11825	in
ryp	1.88963	in
Section Moduli		
Szt	71.4123	in3
Szb	82.3233	in3
Syt	16.0422	in3
Syb	12.9907	in3
Zzp	94.3998	in3
Zyp	20.1841	in3
PNAz	0.507009	in
PNAy	-0.50479	in
PNAzp	0.116033	in
PNAyp	-0.35387	in
Shear Properties		
Az	3.33312	in2
Ay	7.0775	in2
SCz	0.136346	in
SCy	4.81618	in
Qz	46.1717	in3
Qy	11.962	in3
Torsion and Warping Properties		
J	0.605056	in4
r	0.420022	in
Iw	6054.68	in6
βz, pos	-10.3302	in
βy, pos	-1.58538	in
βzp, pos	-9.96654	in
βyp, pos	9.05974	in
Section Capacity		
Ry,base	36	ksi
Mpl,zp	283.199	kip-ft
Mpl,yp	60.5523	kip-ft
Mpl,z	276.743	kip-ft
Mpl,y	63.165	kip-ft
Npl,x	467.047	kip

W21x44

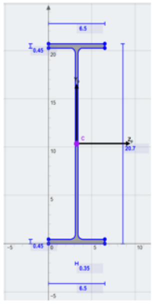

Geometric		
Area	13	in2
Centroidz	3.25	in
Centroidy	10.35	in
Moment of Inertia		
Iz	843	in4
Iy	20.7	in4
Izy	0	in4
rz	8.0752	in
ry	1.2609	in
Section Moduli		
Szt	81.449	in3
Szb	81.449	in3
Syt	6.3692	in3
Syb	6.3692	in3
Zzp	95.4	in3
Zyp	10.2	in3
PNAz	0	in
PNAy	0	in
Shear Properties		
Az	5.3013	in2
Ay	6.976	in2
Apl,z	5.85	in2
Apl,y	7.0875	in2
SCz	0	in
SCy	0	in
Qz	47.915	in3
Qy	5.0907	in3
Torsion and Warping Properties		
J	0.77	in4
r	0.7277	in
Iw	2110	in6
βz, pos	0	in
βy, pos	0	in
Section Capacity		
Ry,base	36	ksi
Mpl,z	287.49	kip-ft
Mpl,y	30.544	kip-ft
Vpl,z	121.52	kip
Vpl,y	147.22	kip
Npl,x	468.53	kip

21ZS4.5/7x0.4375		
Thickness	0.4375	in
Height	21	in
Top Flange	4.5	in
Bottom Flange	7	in
Lips	2	in
Lips Angle	50	deg
Internal Radius	0.6563	in
External Radius	0.875	in
Length	36	in

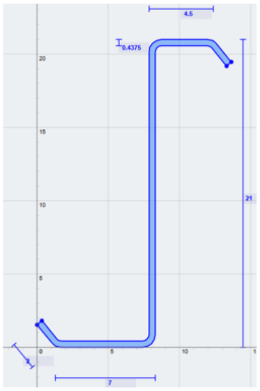

Geometric		
Area	14.997	in2
Centroidz	7.53671	in
Centroidy	9.75017	in
Moment of Inertia		
Iz	918.488	in4
Iy	111.797	in4
Izy	226.619	in4
Izp	977.791	in4
Iyp	52.4935	in4
α	14.6647	°
rz	7.82591	in
ry	2.73032	in
rzp	8.07461	in
ryp	1.8709	in
Section Moduli		
Szt	81.6446	in3
Szb	94.2022	in3
Syt	18.3365	in3
Syb	14.8336	in3
Zzp	108.473	in3
Zyp	23.0944	in3
PNAz	0.502851	in
PNAy	-0.50017	in
PNAzp	0.115298	in
PNAyp	-0.34968	in
Shear Properties		
Az	3.85072	in2
Ay	8.21246	in2
SCz	0.139174	in
SCy	4.83679	in
Qz	53.0607	in3
Qy	13.7251	in3
Torsion and Warping Properties		
J	0.950422	in4
r	0.490556	in
Iw	6785.4	in6
βz, pos	-10.372	in
βy, pos	-1.59226	in
βzp, pos	-10.0095	in
βyp, pos	9.12762	in
Section Capacity		
Ry,base	36	ksi
Mpl,zp	325.419	kip-ft
Mpl,yp	69.2832	kip-ft
Mpl,z	318.036	kip-ft
Mpl,y	72.8265	kip-ft
Npl,x	539.891	kip

W21x50

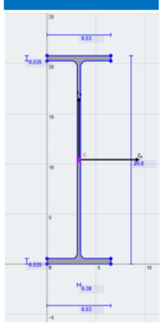

Geometric Properties		
Area	14.7	in2
Centroidz	3.265	in
Centroidy	10.4	in
Moment of Inertia		
Iz	984	in4
Iy	24.9	in4
Izy	0	in4
rz	8.17275	in
ry	1.30157	in
Section Moduli		
Szt	94.6154	in3
Szb	94.6154	in3
Syt	7.62634	in3
Syb	7.62634	in3
Zzp	110	in3
Zyp	12.2	in3
PNAz	0	in
PNAy	0	in
Shear Properties		
Az	6.294	in2
Ay	7.61595	in2
Apl,z	6.9871	in2
Apl,y	7.7007	in2
SCz	0	in
SCy	0	in
Qz	55.0552	in3
Qy	6.09632	in3
Torsion and Warping Properties		
J	1.14	in4
r	0.82099	in
Iw	2570	in6
βz, pos	0	in
βy, pos	0	in
Section Capacity		
Ry,base	36	ksi
Mpl,z	330.331	kip-ft
Mpl,y	36.5778	kip-ft
Vpl,z	145.136	kip
Vpl,y	159.959	kip
Npl,x	530.059	kip

24ZS6/8.5x0.375		
Thickness	0.375	in
Height	24	in
Top Flange	6	in
Bottom Flange	8.5	in
Lips	2	in
Lips Angle	50	deg
Internal Radius	0.5625	in
External Radius	0.75	in
Length	40	in

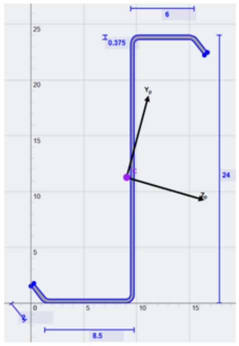

Geometric Properties

Area	15.22	in2
Centroidz	9.054	in
Centroidy	11.27	in

Moment of Inertia

Iz	1268	in4
Iy	171.8	in4
Izy	333.9	in4
Izp	1361	in4
Iyp	78.04	in4
α	15.68	°
rz	9.125	in
ry	3.359	in
rzp	9.457	in
ryp	2.264	in

Section Moduli

Szt	99.61	in3
Szb	112.5	in3
Syt	22.47	in3
Syb	18.97	in3
Zzp	129.1	in3
Zyp	28.61	in3
PNAz	0.524	in
PNAy	-0.523	in
PNAzp	0.111	in
PNAyp	-0.356	in

Shear Properties

Az	4.267	in2
Ay	8.116	in2
SCz	0.156	in
SCy	4.609	in
Qz	62.97	in3
Qy	16.87	in3

Torsion and Warping Properties

J	0.71	in4
r	0.427	in
Iw	14.585 2 x103	in6
βz, pos	-9.914	in
βy, pos	-1.423	in
βzp, pos	-9.524	in
βyp, pos	8.917	in

Section Capacity

Ry,base	36	ksi
Mpl,zp	387.4	kip-ft
Mpl,yp	85.82	kip-ft
Mpl,z	377.5	kip-ft
Mpl,y	90.78	kip-ft
Npl,x	548	

W24x55

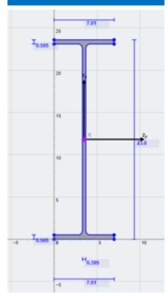

Geometric

Area	16.2	in2
Centroidz	3.505	in
Centroidy	11.8	in

Moment of Inertia

Iz	1350	in4
Iy	29.1	in4
Izy	0	in4
rz	9.129	in
ry	1.339	in

Section Moduli

Szt	114.4	in3
Szb	114.4	in3
Syt	8.302	in3
Syb	8.302	in3
Zzp	134	in3
Zyp	13.3	in3
PNAz	0	in
PNAy	0	in

Shear Properties

Az	6.384	in2
Ay	8.956	in2
Apl,z	7.08	in2
Apl,y	9.123	in2
SCz	0	in
SCy	0	in
Qz	67.41	in3
Qy	6.682	in3

Torsion and Warping

J	1.18	in4
r	0.81	in
Iw	3870	in6
βz, pos	0	in
βy, pos	0	in

Section Capacity

Ry,base	36	ksi
Mpl,z	404.5	kip-ft
Mpl,y	40.09	kip-ft
Vpl,z	147.1	kip
Vpl,y	189.5	kip
Npl,x	584.7	ki

24ZS6/8.5x0.4375		
Thickness	0.4375	in
Height	24	in
Top Flange	6	in
Bottom Flange	8.5	in
Lips	2	in
Lips Angle	50	deg
Internal Radius	0.6563	in
External Radius	0.875	in
Length	40	in

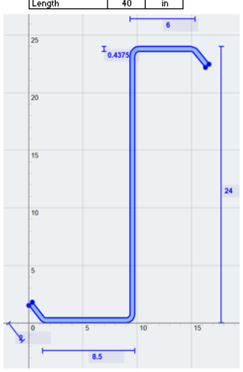

Geometric Properties

Area	17.622	in2
Centroidz	9.0226	in
Centroidy	11.269	in

Moment of Inertia

Iz	1454.5	in4
Iy	196.09	in4
Izy	382.78	in4
Izp	1561.8	in4
Iyp	88.805	in4
α	15.657	°
rz	9.0851	in
ry	3.3358	in
rzp	9.4142	in
ryp	2.2449	in

Section Moduli

Szt	114.25	in3
Szb	129.07	in3
Syt	25.764	in3
Syb	21.734	in3
Zzp	148.72	in3
Zyp	32.828	in3
PNAz	0.5205	in
PNAy	-0.519	in
PNAzp	0.1105	in
PNAyp	-0.353	in

Shear Properties

Az	4.9394	in2
Ay	9.426	in2
SCz	0.1591	in
SCy	4.6288	in
Qz	72.536	in3
Qy	19.401	in3

Torsion and Warping Properties

J	1.118	in4
r	0.4908	in
Iw	16.4723	in6
βz, pos	-9.953	in
βy, pos	-1.425	in
βzp, pos	-9.565	in
βyp, pos	8.974	in

Section Capacity

Ry,base	36	ksi
Mpl,zp	446.16	kip-ft
Mpl,yp	98.484	kip-ft
Mpl,z	434.86	kip-ft
Mpl,y	104.84	kip-ft
Npl,x	634.39	kip

W24x62

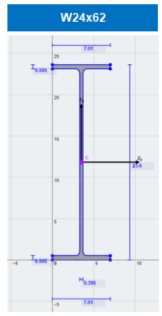

Geometric

Area	18.2	in2
Centroidz	3.52	in
Centroidy	11.85	in

Moment of Inertia

Iz	1550	in4
Iy	34.5	in4
Izy	0	in4
rz	9.2155	in
ry	1.3756	in

Section Moduli

Szt	130.8	in3
Szb	130.8	in3
Syt	9.8011	in3
Syb	9.8011	in3
Zzp	153	in3
Zyp	15.7	in3
PNAz	0	in
PNAy	0	in

Shear Properties

Az	7.4499	in2
Ay	9.791	in2
Apl,z	8.3072	in2
Apl,y	9.9373	in2
SCz	0	in
SCy	0	in
Qz	76.561	in3
Qy	7.8699	in3

Torsion and Warping Properties

J	1.71	in4
r	0.9103	in
Iw	4620	in6
βz, pos	0	in
βy, pos	0	in

Section Capacity

Ry,base	36	ksi
Mpl,z	459.37	kip-ft
Mpl,y	47.219	kip-ft
Vpl,z	172.56	kip
Vpl,y	206.42	kip
Npl,x	656.12	kip